CORRESPONDENCE

Comments on "The Tropospheric Land–Sea Warming Contrast as the Driver of Tropical Sea Level Pressure Changes"

A. M. MAKARIEVA AND V. G. GORSHKOV

Theoretical Physics Division, National Research Centre "Kurchatov Institute" B.P. Konstantinov Petersburg Nuclear Physics Institute, St. Petersburg, Russia, and XIEG-UCR International Center for Arid Land Ecology, University of California, Riverside, Riverside, California

A. V. NEFIODOV

Theoretical Physics Division, National Research Centre "Kurchatov Institute" B.P. Konstantinov Petersburg Nuclear Physics Institute, St. Petersburg, Russia

D. SHEIL

Norwegian University of Life Sciences, Ås, Norway, and School of Environment, Science and Engineering, Southern Cross University, Lismore, New South Wales, Australia, and Center for International Forestry Research, Bogor, Indonesia

A. D. NOBRE

Centro de Ciência do Sistema Terrestre INPE, São José dos Campos, São Paulo, Brazil

B.-L. LI

XIEG-UCR International Center for Arid Land Ecology, University of California, Riverside, Riverside, California

(Manuscript received 26 August 2014, in final form 19 January 2015)

ABSTRACT

In their paper "The tropospheric land–sea warming contrast as the driver of tropical sea level pressure changes," Bayr and Dommenget proposed a simple model of temperature-driven air redistribution to quantify the ratio between changes of sea level pressure p_s and mean tropospheric temperature T_a in the tropics. This model assumes that the height of the tropical troposphere is isobaric. Here problems with this model are identified. A revised relationship between p_s and T_a is derived governed by two parameters—the isobaric and isothermal heights—rather than just one. Further insight is provided by the earlier model of Lindzen and Nigam, which was the first to use the concept of isobaric height to relate tropical p_s to air temperature, and they did this by assuming that isobaric height is always around 3 km and isothermal height is likewise near constant. Observational data, presented here, show that neither of these heights is spatially universal nor does their mean values match previous assumptions. Analyses show that the ratio of the long-term changes in p_s and T_a associated with land–sea temperature contrasts in a warming climate—the focus of Bayr and Dommenget's work—is in fact determined by the corresponding ratio of spatial differences in the annual mean p_s and T_a. The latter ratio, reflecting lower pressure at higher temperature, is significantly impacted by the meridional pressure and temperature differences. Considerations of isobaric heights are shown to be unable to predict either spatial or temporal variation in p_s. As noted by Bayr and Dommenget, the role of moisture dynamics in generating sea level pressure variation remains in need of further theoretical investigations.

1. Introduction

Low-level tropical winds are generally linked to convection, but the physical processes and relationships remain a matter of interest and discussion. Indeed, our incomplete understanding of the physical principles governing low-level circulation is manifested by the inability of atmospheric models to replicate the terrestrial water cycle (Marengo 2006; Hagemann et al. 2011) as well as by the challenge of confidently predicting precipitation and air circulation (e.g., An 2011; Acharya

Corresponding author address: A. M. Makarieva, NRC "Kurchatov Institute" PNPI, 188300, Gatchina, St. Petersburg, Russia.
E-mail: ammakarieva@gmail.com

DOI: 10.1175/JCLI-D-14-00592.1

et al. 2011; Huang et al. 2013). One recurring question is whether the release of latent heat in the upper atmosphere generates sufficient moisture convergence in the lower atmosphere to feed convection. The observed relationship between sea level pressure and surface temperature (with warm areas having low pressure) is regarded as evidence that low-level convergence is, rather, driven by the temperature gradients; see discussions by Lindzen and Nigam (1987), Neelin (1989), Sobel and Neelin (2006), Back and Bretherton (2009), and An (2011).

The physical rationale behind surface pressure gradients driven by surface temperature gradients is that a gaseous atmosphere held by a gravitational field cannot remain static in the presence of a horizontal temperature gradient (Landau and Lifshitz 1987). Any differential heating causes pressure differences in the upper atmosphere to arise as a result of the larger exponential scale height of a warmer versus a colder atmospheric column. As illustrated by the Bjerknes circulation theorem (Thorpe et al. 2003), this implies circulation: upper-level air divergence from the warmer air column and low-level convergence toward it. However, to estimate the strength of this circulation requires a shift from qualitative to quantitative considerations.

The magnitude of the surface pressure gradient can be found if one knows the isobaric height (i.e., the altitude where pressure does not vary over space). Where temperature is high (and air density is low) there is less air below the isobaric height than where temperature is low (and air density is high); this follows from the hypsometric equation, which captures the hydrostatic equation and the ideal gas law. Accordingly, the weight of the air column is lower in warmer than in colder areas. The resulting surface pressure and temperature gradients can be shown to be proportional to each other, with the proportionality coefficient depending on the isobaric height (see section 3).

It thus appears that if we could determine isobaric height from some independent considerations we could use air temperature to predict surface pressures. To address this challenge Bayr and Dommenget (2013), in the context of their efforts to estimate large-scale changes in atmospheric pressure in the tropics during climate change, proposed a highly simplified physical model of temperature-driven air redistribution. The model quantified the relationship between tropical sea level pressure p_s and the mean tropospheric temperature T_a under the assumption that the isobaric height z_e is the height of the troposphere ($z_e = 16.5$ km).

Although not cited by Bayr and Dommenget (2013), Lindzen and Nigam (1987) had previously proposed a similar relationship between p_s and surface temperature T_s by assuming that the tropical isobaric height is around 3 km. This discrepancy requires exploration, because with $z_e = 3$ km the model of Bayr and Dommenget (2013) no longer agrees with observations.

We note too that Lindzen and Nigam (1987) found that isobaric height alone was insufficient to obtain a satisfactory agreement between their model and data. An additional parameter was required. This additional parameter describes the rate at which surface temperature differences diminish with altitude, thereby defining an ''isothermal height'' where no information about the surface temperature differences is preserved. This isothermal height describes horizontal variation in the vertical lapse rate of air temperature. Mean tropospheric temperature investigated by Bayr and Dommenget (2013) should be influenced by such variation even though this is neglected in their simplified model.

Here we reexamine the derivation of Bayr and Dommenget (2013) to identify and resolve several inconsistencies (section 2). We derive a general relationship linking the ratio of horizontal differences of surface pressure and air temperature to isobaric height. We show that, in agreement with the model of Lindzen and Nigam (1987) and in contrast to the model of Bayr and Dommenget (2013), who consider only isobaric height, this ratio is a function of both isobaric and isothermal heights (section 3).

Using data provided by the National Centers for Environmental Prediction–National Center for Atmospheric Research (NCEP–NCAR) reanalysis (Kalnay et al. 1996) and by Remote Sensing Systems (Mears and Wentz 2009) we then assess the isobaric and isothermal heights in the tropics (section 4). We demonstrate in theory that the relationship between sea level pressure and T_a is significantly more sensitive to any changes in isothermal height than is the relationship between p_s and T_s. Accordingly, the ratio $\Delta p_s/\Delta T_a$ is not constant in the tropics and increases by about a factor of 3 from the higher latitudes toward the equator. Meanwhile the ratio $\Delta p_s/\Delta T_s$ is more spatially stable.

While the distinction between spatial and temporal variability was not clearly drawn by Bayr and Dommenget (2013), we show that their data reveal an interesting pattern. The observed long-term temporal changes of sea level pressure and mean tropospheric temperature are characterized by the same ratio as their respective spatial changes. In both cases land displays a smaller (by absolute magnitude) ratio than the ocean. This pattern matches the observations but is not reproduced in the multimodel ensemble of the Intergovernmental Panel on Climate Change (IPCC) (section 5).

Our analysis of the data further reveals that neither of the two assumptions made by Lindzen and Nigam (1987) concerning the isobaric and isothermal heights appears plausible. Isobaric height is highly variable with a different distribution for land and ocean. Isothermal height is also spatially variable. This variability of both parameters prevents confident estimation of the relationship between sea level pressure and temperature from isobaric and isothermal heights (section 6). We conclude with a discussion of possible directions for future research as to how consideration of the relationships between sea level pressure and air temperature could inform our understanding of the principles governing low-level atmospheric circulation and moisture convergence (section 7).

2. The model of Bayr and Dommenget (2013)

Bayr and Dommenget (2013) begin their derivation with an equation they refer to as "the hydrostatic equation":

$$dp = -\rho g d\eta, \tag{1}$$

with pressure p, density ρ, gravity constant g, and η described as "air column height."[1] According to Bayr and Dommenget (2013), for an "isobaric thermal expansion of the air column" it follows from the ideal gas law that

$$d\eta = \frac{\eta}{T} dT, \tag{2}$$

where T is temperature. They conclude that using Eqs. (1) and (2) one obtains how sea level pressure depends on temperature:

$$\frac{dp}{dT} = \frac{1}{2}\rho g \frac{\eta}{T}. \tag{3}$$

We first note that both the ½ multiplier and the lack of the minus sign in Eq. (3) are not consistent with Eqs. (1) and (2). Bayr and Dommenget (2013) explain the appearance of ½ using a graphical scheme that we have redrawn in Fig. 1. They explain that "to balance the heights of the two columns at the end, half of the height difference is moved from the warmer to the colder air volume." As we can see from Fig. 1, this statement refers to the difference in heights η between two local columns. However, to test their model against the data, Bayr and Dommenget (2013) define dp and dT in Eq. (3) to represent the relative changes $d(p_s - \overline{p_s})$ and $d(T_a - \overline{T_a})$, where p_s and T_a are the local values of sea level pressure and mean tropospheric temperature, respectively, and the overbar their mean values in the tropics. If the mean values $\overline{\eta}, \overline{p_s}$, and $\overline{T_a}$ change negligibly in time compared to their local values (i.e., $d\overline{X} \approx 0$ with $X = \{p_s, T_a, \eta\}$), replacement of variables $X \to X - \overline{X}$ does not affect Eqs. (1) and (2). This replacement does, however, impact the balancing procedure in Fig. 1. Indeed, to balance height η between the two columns one has to move not one-half but the *entire* difference $d(\eta - \overline{\eta}) = (\eta_1 - \eta_2)/2$ from the warmer to the colder column. Therefore, if by dp/dT in Eq. (3) one understands, as do Bayr and Dommenget (2013), relative changes of the respective variables, one has no grounds to introduce the ½ multiplier into Eq. (3) [see Eq. (20) in the next section].

The sign discrepancy between Eqs. (1) and (3) appears as a simple error, but in fact it manifests the misapplication of Eq. (1). This equation is not a hydrostatic equation and contradicts the latter. Let us illustrate this point. For atmospheric air conforming to the ideal gas law

$$p = NRT, \tag{4}$$

where $R = 8.3\,\mathrm{J\,mol^{-1}\,K^{-1}}$ and N is molar density, the hydrostatic equilibrium equation is

$$\frac{\partial p(z)}{\partial z} = -\rho(z)g = -\frac{p}{h} \quad \text{and} \quad h \equiv \frac{RT(z)}{Mg}, \tag{5}$$

where M is molar mass, z is height above the sea level, and p, ρ, and T are local values of pressure, density, and temperature at height z. The hydrostatic equilibrium Eq. (5) says nothing about temporal changes of either pressure or temperature. It only describes the distribution of air pressure with height.

In Eqs. (1)–(3) Bayr and Dommenget (2013) interpreted pressure p as sea level pressure $p = p_s$, density ρ as the mean air density in the troposphere $\rho = \rho_a = 0.562\,\mathrm{kg\,m^{-3}}$ and air column height η as the height $H = 16.5\,\mathrm{km}$ of the tropical troposphere corresponding to height η_{100} of pressure level $p_{100} = 100\,\mathrm{hPa}$. They also interpreted differentials in Eqs. (1)–(3) as describing temporal changes of the corresponding variables. From Eq. (5) we find that sea level pressure p_s is related to ρ_a and η_{100} as follows:

$$p_s \equiv \int_0^\infty \rho g\, dz = \rho_a g \eta_{100} + p_{100} \quad \text{and}$$
$$\rho_a \equiv \frac{1}{\eta_{100}} \int_0^{\eta_{100}} \rho(z)\, dz. \tag{6}$$

Taking differential of Eq. (6) we obtain

$$dp_s = \rho_a g d\eta_{100} + g\eta_{100} d\rho_a. \tag{7}$$

[1] In the derivation of Bayr and Dommenget (2013) η in Eq. (1) is denoted as h.

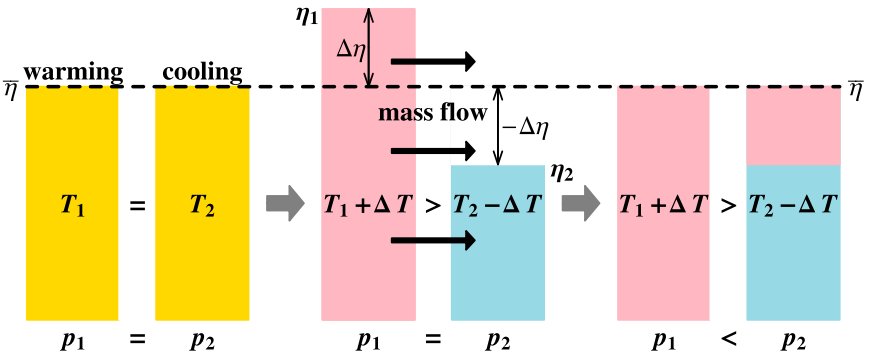

FIG. 1. Schematic of the physical model of Bayr and Dommenget (2013) with a constant mean column height $\overline{\eta}$ [redrawn from Fig. 4 of Bayr and Dommenget (2013)]. To balance two columns of heights η_1 and η_2, one should either move to the second column from the first column half of the total height difference $\eta_1 - \eta_2$ or the entire difference $\Delta\eta \equiv \eta_1 - \overline{\eta}$ between η_1 and the mean height $\overline{\eta} \equiv (\eta_1 + \eta_2)/2$.

When we compare Eqs. (7) and (1) with $p = p_s$, $\rho = \rho_a$, and $\eta = \eta_{100}$ it is apparent that in Eq. (1) the minus sign was incorrectly added to the first term in Eq. (7). The second term in Eq. (7), compressibility of the atmospheric air $d\rho_a \neq 0$, was dropped altogether.

For an incompressible fluid with $\rho = \rho_a = \text{constant}$, Eq. (7) has the familiar meaning relating column height to surface pressure: the larger the height of the fluid column, the higher the surface pressure. Meanwhile the minus sign in Eq. (1) presumes exactly the opposite: the larger the column height η, the smaller the surface pressure. On the other hand, if Bayr and Dommenget (2013), having ignored air compressibility for an unknown reason, used Eq. (1) with the plus sign, the sign discrepancy between Eqs. (3) and (1) would have disappeared. However, in this case Eq. (3) would have yielded a positive relationship of surface pressure on temperature (higher pressure at larger temperature), which contradicts the observations: in the real atmosphere lower sea level pressure is associated with higher temperature.

As the model of Bayr and Dommenget (2013) is based on incorrect relationship [Eq. (1)] we conclude that it lacks explanatory power and matches observations by chance alone.

3. Dependence of sea level pressure on temperature

We will here derive a general relationship linking surface pressure and temperature to the vertical structure of the atmosphere. The model of Bayr and Dommenget (2013) neglects how temperature might vary with altitude. We will allow air temperature to vary with height with a lapse rate $\Gamma \equiv -\partial T/\partial z$, which is independent of height but can vary in the horizontal direction.

We introduce the following dimensionless variables to replace height z and lapse rate Γ:

$$Z \equiv \frac{z}{h_s}, \quad c \equiv \frac{\Gamma}{\Gamma_g}, \quad h_s \equiv \frac{RT_s}{Mg} \equiv \frac{T_s}{\Gamma_g}, \quad \text{and} \quad \Gamma_g \equiv \frac{Mg}{R}, \tag{8}$$

where $M = 29\,\text{g mol}^{-1}$ and $\Gamma_g = 34\,\text{K km}^{-1}$ is the so-called autoconvective lapse rate.

For air temperature we have

$$T(Z) = T_s(1 - cZ), \tag{9}$$

where $Z < c^{-1}$ and $T_s \equiv T(0)$. In these variables the hydrostatic equilibrium Eq. (5) assumes the form

$$-\frac{\partial p}{\partial Z} = \rho g h_s = \frac{p}{1 - cZ}. \tag{10}$$

Solving Eq. (10) for $p \geq 0$ we have

$$\ln\frac{p}{p_s} = -\int_0^Z \frac{dZ'}{1 - cZ'} = \frac{1}{c}\ln(1 - cZ) \approx -Z\left(1 + \frac{1}{2}cZ\right). \tag{11}$$

The approximate equality in Eq. (11) holds for $cZ < 1$, which for $\Gamma \approx 6\,\text{K km}^{-1}$ corresponds to $Z \leq c^{-1} = 5.7$. This is always the case in the troposphere, where $z \leq 17\,\text{km}$ and $Z < 2$ (for $h_s = 8.7\,\text{km}$). Comparison with the exact formula reveals that the maximum inaccuracy of the approximate relationship in Eq. (11) corresponds to the top of the troposphere where it amounts to 4%.

If one neglects the quadratic term in the right-hand side of Eq. (11) one obtains the well-known hypsometric equation relating the ratio between surface pressure p_s and pressure level p to height z of pressure level p. This equation does not depend on c and thus neglects the dependence of temperature on height. This is justified for small height differences but not for the entire troposphere where for $Z = 2$ the second (quadratic) term in the right-hand side of Eq. (11) can make up to 18% of the first (linear) term and thus cannot be neglected.

Pressure $p(z)$ and temperature $T(z)$ at a given height z are functions of p_s, T_s, and Γ. Considering linear deviations from the mean values of $\overline{p_s}$, $\overline{T_s}$, and $\overline{\Gamma}$ and taking the total differential of the approximate relationship for p [Eq. (11)] over these three variables, we obtain

$$dp = p_s\left(da + Zdb - \frac{1}{2}Z^2dc\right)e^{-Z}, \tag{12}$$

where da, db, and dc stand for the dimensionless differentials of p_s, T_s and Γ:

$$da \equiv \frac{dp_s}{p_s} \approx \frac{dp_s}{\overline{p_s}}, \quad db \equiv \frac{dT_s}{T_s} \approx \frac{dT_s}{\overline{T_s}}, \quad \text{and}$$
$$dc \equiv \frac{d\Gamma}{\Gamma_g}, \tag{13}$$

where $\overline{p_s}$ = 1013 hPa and $\overline{T_s}$ = 298 K are the annual mean sea level pressure and surface air temperature in the tropics. The inaccuracy of the approximate relationships in Eq. (13) is determined by the relative changes of sea level pressure and surface temperature across the tropics. For the zonally averaged p_s and T_s this inaccuracy does not exceed 4%.

Isothermal height $z_i = Z_i h_s$ is found by taking total differential of T [Eq. (9)] over T_s and Γ and putting $dT = dT_s - T_s Z_i dc = 0$. This gives

$$Z_i = \frac{db}{dc} = \frac{1}{h_s}\frac{dT_s}{d\Gamma} \quad \text{and} \quad z_i \equiv Z_i h_s = \frac{dT_s}{d\Gamma}. \tag{14}$$

We can see from Eq. (14) that an isothermal height exists if only $db/dc > 0$ (i.e., if areas with a warmer surface have a higher lapse rate). Bayr and Dommenget (2013) note that this pattern should be related to moisture availability. They note too that, below an isothermal surface, drier areas should have a steeper lapse rate close to the dry adiabat and thus get warmer than moist areas where the lapse rate is lower because of latent heat release. In the tropical atmosphere, moist areas, most notably the equatorial regions, have on average a steeper mean tropospheric lapse rate than do the drier regions at higher tropical latitudes (e.g., Johnson et al. 1999, their Fig. 13). In the lower atmosphere this has to do with the trade wind inversion, which is mostly pronounced in the drier (colder) regions where the lapse rate in the low atmosphere is very small. In the upper troposphere (around the isothermal height) a higher lapse rate in the moister regions is due to the fact that in such regions the air ascends rapidly and thus has a lapse rate closer to adiabatic than in the slowly descending air, where a more significant part of the thermal energy can be radiated to space. It is only in the middle atmosphere that, because of latent heat release, the lapse rate over the moist equatorial areas is smaller than it is at higher tropical latitudes. Generally, both in the lower atmosphere and on average in the troposphere $db/dc > 0$ is fulfilled.

Isobaric height $z_e \equiv Z_e h_s$ is defined from Eq. (12) as the height where $dp = 0$. It is determined from the following quadratic equation:

$$da + Z_e db - \frac{1}{2}Z_e^2 dc = 0 \quad \text{and}$$
$$Z_e = Z_i\left[1 \pm \left(1 + \frac{2}{Z_i}\frac{da}{db}\right)^{1/2}\right]. \tag{15}$$

As there can be two solutions there can be two isobaric heights (Fig. 2). Note that the isobaric height Z_e [Eq. (15)] does not depend on lapse rate c but only on its differential dc via Z_i. This is a consequence of the smallness of $cZ \ll 1$ in the troposphere. From Eqs. (15) and (14) we obtain the following relationship for the ratio of the differentials of surface pressure and temperature [Eq. (13)]:

$$\frac{da}{db} = -Z_e\left(1 - \frac{1}{2}\frac{Z_e}{Z_i}\right). \tag{16}$$

When $db = 0$ (i.e., when the surface temperature does not vary, but only lapse rate does), we have from Eq. (15)

$$\frac{da}{dc} = \frac{Z_e^2}{2}. \tag{17}$$

The surface pressure change is proportional to the change in lapse rate; that is, the pressure is lower where the lapse rate is smaller, with the proportionality coefficient equal to half the squared isobaric height.

To find the relationship between the isobaric height and mean tropospheric temperature T_a below the 100-hPa level we need to find the relationship between T_a and T_s. This relationship takes the form (see the appendix)

$$\frac{db}{dn} = \frac{1}{1 - 0.66/Z_i} \quad \text{and} \quad dn \equiv \frac{dT_a}{T_a}. \tag{18}$$

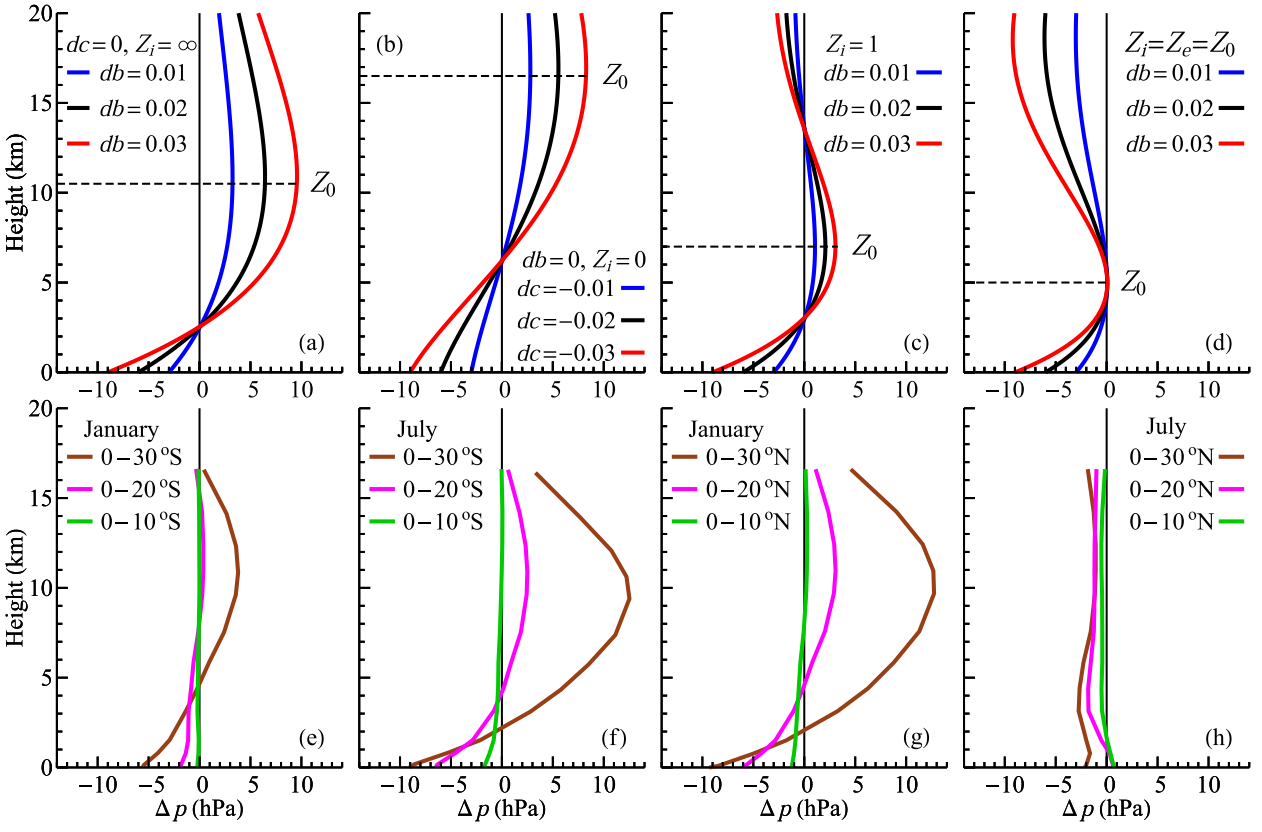

FIG. 2. Vertical profiles of pressure differences $\Delta p(z)$ between air columns differing in their lapse rate, surface pressure, and temperature. (a)–(d) Theoretical profiles with $dp = \Delta p$ [Eq. (12)], where $da = \Delta p_s/p_s$, $db = \Delta T_s/T_s$, and $dc = \Delta\Gamma/\Gamma_g$ [cf. Eq. (13)], and $p_s = 1000$ hPa and $T_s = 300$ K. In (a)–(d) $da = -0.003$, -0.006, and -0.009 for the blue, black, and red curves, respectively. In each panel da/db = const for all the three curves. Dashed line Z_0 [Eq. (21)] shows the height where the positive pressure difference in the upper atmosphere is maximum, $\Delta p(Z_0) = \Delta p_0$ [Eq. (22)]. Note two isobaric heights in (c). In (d) the condition $Z_i = Z_0$ (the atmosphere is horizontally isothermal where the positive pressure difference aloft is maximum) yields $Z_i = Z_0 = Z_e = -2da/db = (-2da/dc)^{1/2}$ [see Eqs. (15), (21), and (14)] and $\Delta p_0 = 0$ (i.e., the pressure surplus aloft disappears). Also shown are the real vertical profiles of zonally averaged pressure differences between the air columns at the equator and 10°, 20°, and 30° latitude in the (e),(f) Southern and (g),(h) Northern Hemispheres in (e),(g) January and (f),(h) July; for example, the brown line in (e) shows the difference between the air column at the equator and at 30°S in January. Note that while the theoretical curves in (a)–(d) are chosen such that they have one and the same isobaric height Z_e (i.e., they cross the line $\Delta p = 0$ at the same point), this varies for the real profiles in (e)–(h).

Finally from Eqs. (16) and (18) we obtain

$$\frac{da}{dn} = -Z_e\left(1 - \frac{1}{2}\frac{Z_e}{Z_i}\right)\frac{1}{1 - 0.66/Z_i}. \tag{19}$$

Equations (16) and (19) are shown in Fig. 3.

When, as in the model of Bayr and Dommenget (2013), lapse rate is assumed to be constant with $dc = 0$, we have $Z_i = \infty$ and Eq. (19), using notations from Eq. (13) and $dn \equiv dT_a/T_a$, becomes

$$\frac{da}{db} = \frac{da}{dn} = -Z_e \quad \text{and}$$
$$\frac{dp_s}{dT_a} = -\frac{z_e}{h_s}\frac{p_s}{T_a} = -\rho_s g\frac{z_e}{T_a}. \tag{20}$$

Comparing Eq. (20) to Eq. (3) of Bayr and Dommenget (2013) we notice the absence of the coefficient ½ in Eq. (20) and the presence of surface air density ρ_s in Eq. (20) instead of mean tropospheric air density $\rho = \rho_a$ in Eq. (3). If the lapse rate did not vary in the horizontal plane, Eq. (20) would be the correct equation relating ratio of pressure and temperature differences to an isobaric height. But as we will show below, in the real atmosphere variation in the lapse rate is too influential to ignore.

Considering $dp = \Delta p(z)$ in Eq. (12) as a small pressure difference at a given height between two air columns, we note that this difference has a maximum above the isobaric height Z_e [Eq. (15)] at a certain height Z_0. This height is determined by taking the derivative of Eq. (12) over Z and equating it to zero [see Eqs. (12), (15) and (14)]:

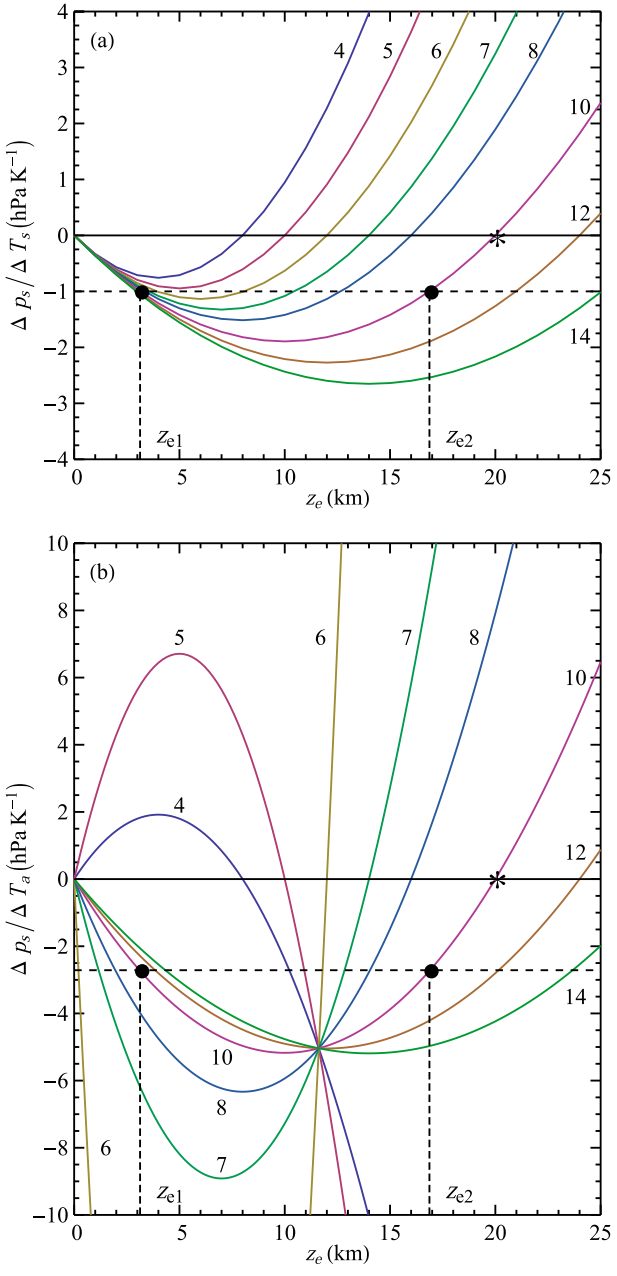

FIG. 3. Dependence of (a) $\Delta p_s/\Delta T_s$ [Eq. (16)] and (b) $\Delta p_s/\Delta T_a$ [Eqs. (19) and (23)] on isobaric height z_e for different values of isothermal height z_i (km) that are shown near the corresponding curves. Vertical dashed lines denote isobaric heights z_{e1} and z_{e2} corresponding to the tropical mean $\Delta p_s/\Delta T_s = -1$ hPa K^{-1} [horizontal dashed line in (a); Fig. 4d] for $z_i = 10$ km. With an increase in z_{e2} from 17 to 20 km for $z_i = 10$ km both $\Delta p_s/\Delta T_s$ and $\Delta p_s/\Delta T_a$ become zero (shown with asterisks).

$$\frac{\partial \Delta p}{\partial Z} = 0, \quad da + Z_0 db - \frac{1}{2} Z_0^2 dc - db + Z_0 dc = 0, \quad \text{and}$$
$$Z_0 = 1 + Z_i \pm [(Z_e - Z_i)^2 + 1]^{1/2}. \tag{21}$$

At this height the pressure difference is equal to

$$\Delta p_0 \equiv \Delta p(Z_0) = p_s e^{-Z_0}\left(da + Z_0 db - \frac{1}{2} Z_0^2 dc\right)$$
$$= p_s e^{-Z_0}(db - Z_0 dc). \tag{22}$$

Note that by definition when $\Delta p_0 = 0$ we have $Z_e = Z_0 = Z_i$. As is clear from Fig. 2, where the vertical profiles of $\Delta p(z)$ [Eq. (12)] are shown for different values of da, db, and dc, Δp_0 is the maximum pressure difference between the air columns above the lower isobaric height.

As follows from Eqs. (21), (22), and (16), height Z_0 as well as the ratio between the pressure surplus aloft and the pressure shortage at the surface $\Delta p_0/\Delta p_s$ are functions of two parameters, the isobaric and isothermal heights Z_e and Z_i. When Z_e and Z_i are constant, the ratio between the pressure surplus aloft and the pressure shortage at the surface in the warmer column is constant as well: the larger the pressure surplus aloft, the larger the surface pressure shortage, with a direct proportionality between the two. This is consistent with the conventional thinking about differential heating, namely that the upper pressure surplus causes air to diverge from the warmer column, the total amount of gas will diminish, and there appears a shortage of pressure at the surface $\Delta p_s < 0$ (e.g., Pielke 1981, his Fig. 2).

When the vertical lapse rate is constant, $dc = 0$, from Eq. (21) we have $Z_0 = 1 - da/db$. In this case, as is clear from Eq. (22), for small values of $da/db \ll 1$ the magnitude of Δp_0 does not depend on da but is directly proportional to db, that is, to ΔT_s [Eq. (13); Fig. 2a]. This means that under these particular conditions a surface temperature gradient directly determines the pressure gradient *in the upper atmosphere.* In this sense there is no difference between surface temperature gradient and a gradient of lapse rate related to latent heat release; both can only determine a pressure surplus aloft (cf. Figs. 2a,b). We emphasize that while under certain assumptions the magnitude of the tropospheric pressure gradient can be approximately specified from considerations of the hydrostatic balance and air temperature gradients alone, the magnitude of the surface pressure gradient cannot.

Generally, ratios da/db and db/dc in Eqs. (15) and (14) can be understood as the ratios of the gradients of the corresponding variables, for example, $da/db = (\partial p_s/\partial y)/(\partial T_s/\partial y)(T_s/p_s)$, where $(\partial p_s/\partial y)/(\partial T_s/\partial y)$ is the ratio of sea level pressure and surface temperature gradients in a given y direction (e.g., along the meridian). In this case for any y the value of z_e (or z_i) has the meaning of a height where $\partial p/\partial y = 0$ (or $\partial T/\partial y = 0$), that is, where pressure (or air temperature) does not vary over y. These ratios can also be understood as the ratios of small

finite differences between pressure or temperature in a given grid point and a certain reference value of pressure or temperature, $dp_s/dT_s = \Delta p_s/\Delta T_s$. This approach was taken by Lindzen and Nigam (1987) and Bayr and Dommenget (2013). We can now estimate all parameters in Eq. (19) from empirical data to compare them with model assumptions.

4. Data

We used NCEP–NCAR reanalysis data on sea level pressure and surface air temperature, as well as on geopotential height and air temperature at 13 pressure levels provided by the NOAA/OAR/ESRL PSD, Boulder, Colorado, from their website at http://www.esrl.noaa.gov/psd/ (Kalnay et al. 1996). As an estimate of the mean tropospheric temperature we took temperature total troposphere (TTT) MSU/AMSU satellite data provided by Remote Sensing Systems from their website at http://www.remss.com/measurements/upper-air-temperature (Mears and Wentz 2009). Monthly values of all variables were averaged over the time period from 1978 (the starting year for the TTT data) to 2013 to obtain 12 mean monthly values and one annual mean for each variable for each grid point on a regular 2.5° × 2.5° global grid.[2] The following pressure levels covering the tropical troposphere were considered: 1000, 925, 850, 700, 600, 500, 400, 300, 250, 200, 150, 100, and 70 hPa. Meridional gradients $\partial X/\partial y$ of variable X ($X = \{p_s, T_s\}$) at latitude y were determined as the difference in X values at two neighboring latitudes and dividing by 2.5°: $\partial X(y)/\partial y \equiv [X(y + 1.25°) - X(y - 1.25°)]/2.5°$. Local pressure differences corresponding to pressure level p_j were calculated from the geopotential height differences using the hypsometric equation $\Delta p_j = (z_j - \overline{z_j})p_j/h_j$, where z_j is the local geopotential height of pressure level p_j, $\overline{z_j}$ is its mean value in the considered spatial domain, $h_j = RT_j/(Mg)$ is the local exponential pressure scale height [Eq. (5)], and T_j is local air temperature at this level.

[2] TTT data array contains 144 (360°/2.5°) longitude and 72 (180°/2.5°) latitude values each pertaining to the center of the corresponding grid point. NCEP–NCAR data arrays contain 144 longitude and 73 latitude values each pertaining to the border of the corresponding grid point. For example, the northernmost latitude in the NCEP–NCAR data is 90°N, while for the TTT data it is 90° − 2.5°/2 = 88.75°N. This discrepancy was formally resolved by adding an empty line to the end of the TTT data such that the number of lines matches and there are matching (i, j) grid points in the two arrays. In the result, every TTT value refers to a point in space that is 1.25° to the south and to the east from the coordinate of the corresponding NCEP–NCAR value. This relatively small discrepancy did not appear to have any impact on any of the resulting quantitative conclusions (i.e., if instead one moves TTT points to the north, the results are unchanged).

5. Spatial patterns

Our regression of the annual mean values of $\Delta p_s \equiv p_s - \overline{p_s}$ on $\Delta T_a \equiv T_a - \overline{T_a}$ (the overbars denote spatial averaging) for the tropical area between 22.5°S and 22.5°N produced a slope of $r = -2.3\,\mathrm{hPa\,K^{-1}}$ with $R^2 = 0.75$. This is practically identical to the regression shown in Fig. 3 of Bayr and Dommenget (2013), where Δp_s and ΔT_a values for the four seasons are plotted together. The resulting regression slope $r = -2.4\,\mathrm{hPa\,K^{-1}}$ with $R^2 = 0.76$ was interpreted by Bayr and Dommenget (2013) as describing seasonal changes of sea level pressure and tropospheric temperature. However, as our result shows, even if seasonal changes of $\Delta p_s/\Delta T_a$ were completely absent, the corresponding regression for the four seasons combined would nevertheless produce a nonzero slope reflecting the time-invariable spatial association between higher temperature and lower pressure in the tropics. The agreement between our relationship for the annually averaged Δp_s and ΔT_a ratio and the one shown in Fig. 3 of Bayr and Dommenget (2013) indicates that either the spatial variation dominates the seasonal changes or that the seasonal changes are, on average, characterized by a $\Delta p_s/\Delta T_a$ ratio similar to that of the spatial changes. Bayr and Dommenget (2013) did not discuss whether their Fig. 3 actually characterizes spatial or temporal variation but interpreted the regression shown in their Fig. 3 as a test of validity of their model, which they later used to assess long-term temporal changes in p_s and T_a.

The spatial and temporal changes are not independent. If in a certain area we have an isobaric surface at height z_e and an isothermal surface at height z_i, we have [see Eq. (19)]

$$\Delta p_s = r\Delta T_a \quad \text{and} \quad r \equiv -\frac{z_e}{h_s}\frac{p_s}{T_a}\left(1-\frac{z_e}{2z_i}\right)\frac{1}{1-0.66h_s/z_i}. \tag{23}$$

Local values of $\Delta p_s \equiv p_s - \overline{p_s}$ and $\Delta T_a \equiv T_a - \overline{T_a}$ are defined with respect to their mean values in the area where the isobaric and isothermal surfaces exist. Taking the derivative of Eq. (23) over time we obtain

$$\frac{\partial \Delta p_s}{\partial t} = r\frac{\partial \Delta T_a}{\partial t} \quad \text{if} \quad \frac{\partial r}{\partial t} = 0 \quad \text{and} \quad \frac{\partial \Delta X}{\partial t} \equiv \frac{\partial X}{\partial t} - \frac{\partial \overline{X}}{\partial t}, \tag{24}$$

where $X = \{p_s, T_a\}$.

This means that if z_e, z_i, and, hence, r (to the accuracy of a few percent) do not change with time, then the temporal changes of Δp_s and ΔT_a are characterized by the same ratio r as their spatial changes.

In their analysis of the observed long-term p_s and T_a changes Bayr and Dommenget (2013) compared relative partial pressures and relative tropospheric temperatures in 1989–2010 (their Fig. 12). They found that, in agreement with Eq. (24), these changes are related by practically identical ratios, $-2.0\,\mathrm{hPa\,K^{-1}}$ for land, $-2.4\,\mathrm{hPa\,K^{-1}}$ for ocean, and $-2.3\,\mathrm{hPa\,K^{-1}}$ for tropics as a whole, as the corresponding spatial contrasts shown in Fig. 4a. This pattern is not preserved in the IPCC multimodel ensemble (Bayr and Dommenget 2013, their Fig. 5): modeled long-term changes for the time period 1970–2099 are characterized by a lower ratio for land ($-2.5\,\mathrm{hPa\,K^{-1}}$) than for the ocean ($-1.9\,\mathrm{hPa\,K^{-1}}$) with an overall mean of $-2.0\,\mathrm{hPa\,K^{-1}}$. This discrepancy merits further investigations.

We further found that the regression slope r depends strongly on the averaging domain: it increases by absolute magnitude toward the equator (Fig. 4a). As r decreases with diminishing tropical area, so does the squared correlation coefficient (Fig. 4b), although for the oceanic grid points it remains relatively high even near the equator. For example, for the area between 30°S and 30°N for the land and ocean combined we have $r = -1.5\,\mathrm{hPa\,K^{-1}}$ with $R^2 = 0.73$ while for 5°S and 5°N we have $r = -3.6\,\mathrm{hPa\,K^{-1}}$ with $R^2 = 0.32$. These patterns testify that the spatial relationship between Δp_s and ΔT_a is not universal in the tropics. In contrast, while similar regressions of Δp_s on surface temperature ΔT_a are characterized by lower R^2, the regression slope, around $-1\,\mathrm{hPa\,K^{-1}}$, does not appear to depend significantly on the averaging domain (Figs. 4d,e).

To explore whether the relationship between Δp_s and ΔT_a is dominated by zonal or meridional differences, we performed a regression of zonally averaged Δp_s on zonally averaged ΔT_a for the area between 22.5°S and 22.5°N for different months (Fig. 4c). Zonally averaged values account for a major part of the dependence between Δp_s and ΔT_a: regression of annual mean zonally averaged values yields $r = -2.0\,\mathrm{hPa\,K^{-1}}$. The same is true for the surface temperature (Fig. 4f). Since land–sea contrasts in the tropics are predominantly zonal, this means that either the contribution of land–sea pressure–temperature contrasts to the pantropical regressions of Δp_s on ΔT_a and ΔT_s is relatively unimportant[3] or that these contrasts are characterized by approximately the same ratio as the zonally averaged values.

[3] This conclusion would not imply that the land–ocean contrasts are negligible on a regional scale.

6. Isobaric and isothermal heights and their variability

While the models of Lindzen and Nigam (1987) and Bayr and Dommenget (2013) build upon the notion of an isobaric height, neither study provided a systematic assessment of the observational evidence to quantify its magnitude and variation in space and time. In their model Lindzen and Nigam (1987) adopted a constant isothermal height equal to 10 km. [They assumed that the horizontal temperature differences at the level of $z_{\mathrm{LN}} = 3$ km are 30% smaller than the corresponding differences at the sea level: $\Delta T(z_{\mathrm{LN}}) = 0.7\Delta T_s$. From $\Delta T(z_{\mathrm{LN}}) = T_s - \Gamma z_{\mathrm{LN}}$ and Eq. (14) we obtain $z_i \equiv \Delta T_s/\Delta\Gamma = z_{\mathrm{LN}}/0.3 = 10$ km.]

Generally, a pantropical isobaric (isothermal) height, if it exists, has the following properties: at this height 1) deviation of local pressure (temperature) from the pantropical mean is zero, 2) deviation of local pressure (temperature) from the zonal mean is zero, and 3) local horizontal gradient of pressure (temperature) is zero. If a universal isobaric height does not exist, for each grid point these properties can each define a different height. In Figs. 5a and 5d we plotted zonal averages of the minimal isobaric and isothermal heights calculated according to the above definitions. Local vertical profiles of pressure and temperature differences in individual grid points illustrating how these heights were calculated are exemplified in Figs. 5b and 5e.

In the majority of grid points there is an isobaric height between 0 and 10 km (Fig. 5c), which corresponds to the lower isobaric height from Eq. (15). It is of interest that the land and the ocean have different lower isobaric heights, with land values peaking below the trade wind inversion layer (3 km) and ocean values peaking at around 6 km (Fig. 5c). As is clear from Fig. 5f, a significant part of grid points has two isothermal heights: one is the pantropical isothermal height around 12 km and the second one is around 3 km.

While our Eq. (19) has the limitation of not accounting for the vertical changes in lapse rate, it does provide an insight into the observed behavior of the $\Delta p_s/\Delta T_s$ and $\Delta p_s/\Delta T_a$ ratios. From Fig. 3a we can see that $\Delta p_s/\Delta T_s$ grows with increasing lower isobaric height z_{e1} and, for a given z_e, declines with decreasing isothermal height z_i. As there is a tendency for z_{e1} to grow and for z_i to diminish toward the equator (Figs. 5a,d), this compensating behavior may explain the approximate constancy of $\Delta p_s/\Delta T_s$ (Fig. 4d). Meanwhile, because of the singularity for $z_i \approx 6$ km, a decrease in z_i for $z_e \approx 5$–8 km, in contrast, leads to a sharp increase in $|\Delta p_s/\Delta T_a|$. This theoretical behavior is consistent with the observed growth of $|\Delta p_s/\Delta T_a|$ in the vicinity of the equator (Fig. 4a).

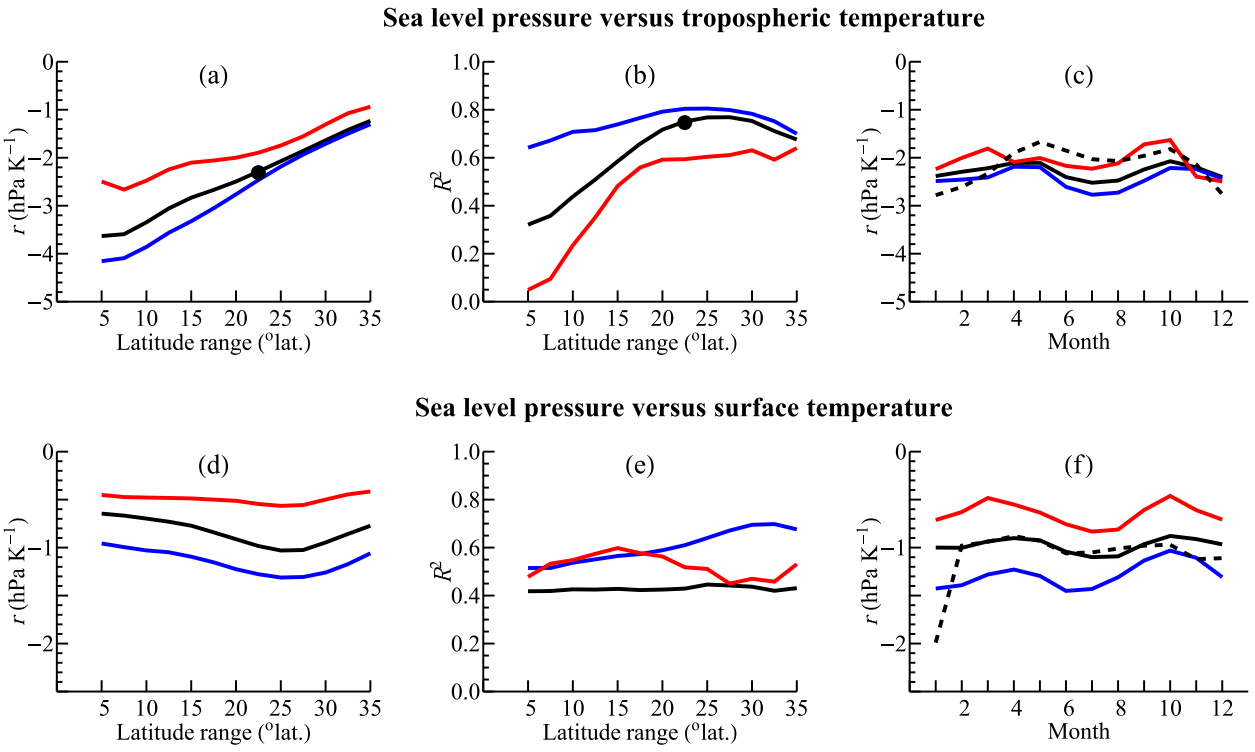

FIG. 4. Regression slopes r and R^2 for the regression (a),(b) $\Delta p_s = r\Delta T_a$ and (d),(e) $\Delta p_s = r\Delta T_s$ for land (red), ocean (blue), and total area (black) as dependent on the considered latitude range. For example, latitude range of 35° means that averaging is made from 35°S to 35°N. Here $\Delta X \equiv X - \overline{X}$ ($X = \{p_s, T_a, T_s\}$), where X is the local annual mean value and $\overline{X}$ is its spatial average over the considered latitude range. Data corresponding to Fig. 3 of Bayr and Dommenget (2013) are marked with black circle. (c),(f) Seasonal variation of r for the latitude range 22.5°S–22.5°N: land (red), ocean (blue), and total tropics (black) curves denote results as in (a) and (d) but for particular months; the dashed line denotes the regression slope of zonally averaged Δp_s with ΔT_a and ΔT_s in (c) and (f), respectively.

Figure 3 also illustrates the sensitivity of these ratios to the values of the lower and upper isobaric heights z_{e1} and z_{e2}. With $z_{e1} \ll z_i$ the ratio of $\Delta p_s/\Delta T_a$ grows approximately proportional to z_{e1}. Accordingly, the land with its significantly lower z_{e1} has lower $\Delta p_s/\Delta T_a$ and $\Delta p_s/\Delta T_s$ than the ocean (Fig. 4a). Thus the observed variability in the lower isobaric height produces uncertainties on the order of 100% in the corresponding estimates of those ratios. While the upper isobaric height appears more conservative, the sensitivity of $\Delta p_s/\Delta T_a$ to its value is much higher. For example, for $z_i = 10$ km a change in z_{e2} of about 10% from 18 to 20 km diminishes the magnitude of $|\Delta p_s/\Delta T_a|$ by more than an order of magnitude (Fig. 3b).

7. Discussion

The simple model of Bayr and Dommenget (2013) was intended as a rough and ready means to capture the dominant features of how tropical air pressure contrasts are determined in a transparent and tractable manner. We have reexamined this model and found that for an atmosphere where the lapse rate is everywhere the same, the correct expression for the dependence between sea level pressure and tropospheric temperature is given by Eq. (20): it differs from Eq. (3) of Bayr and Dommenget (2013) by the absence of ½ and the presence of surface air density ρ_s instead of mean tropospheric density ρ_a. Equation (20) is similar to Eq. (3) in that it describes a direct proportionality between the isobaric height z_e and the $\Delta p_s/\Delta T_a$ ratio.

In the real atmosphere the lapse rate varies considerably in the horizontal plane: the lapse rate over the warmer surfaces is on average steeper than over the colder surfaces especially in the lower atmosphere (Lindzen and Nigam 1987; Johnson et al. 1999). We have shown that in such an atmosphere there must be at least two isobaric heights $z_{e1} \le z_{e2}$ [Eq. (15); Fig. 2c]. The models of Lindzen and Nigam (1987) and Bayr and Dommenget (2013) each considered only one isobaric height. In agreement with our Eq. (15), observations show that in the tropical atmosphere the two isobaric heights correspond to $z_{e1} \sim$ 1.5–6.0 km and $z_{e2} \sim$ 17–20 km. Both heights are spatially variable (Figs. 5a–c). Observations provide no evidence of a near-constant pantropical isobaric height, either around 3 km (Lindzen and Nigam 1987) or at the top of

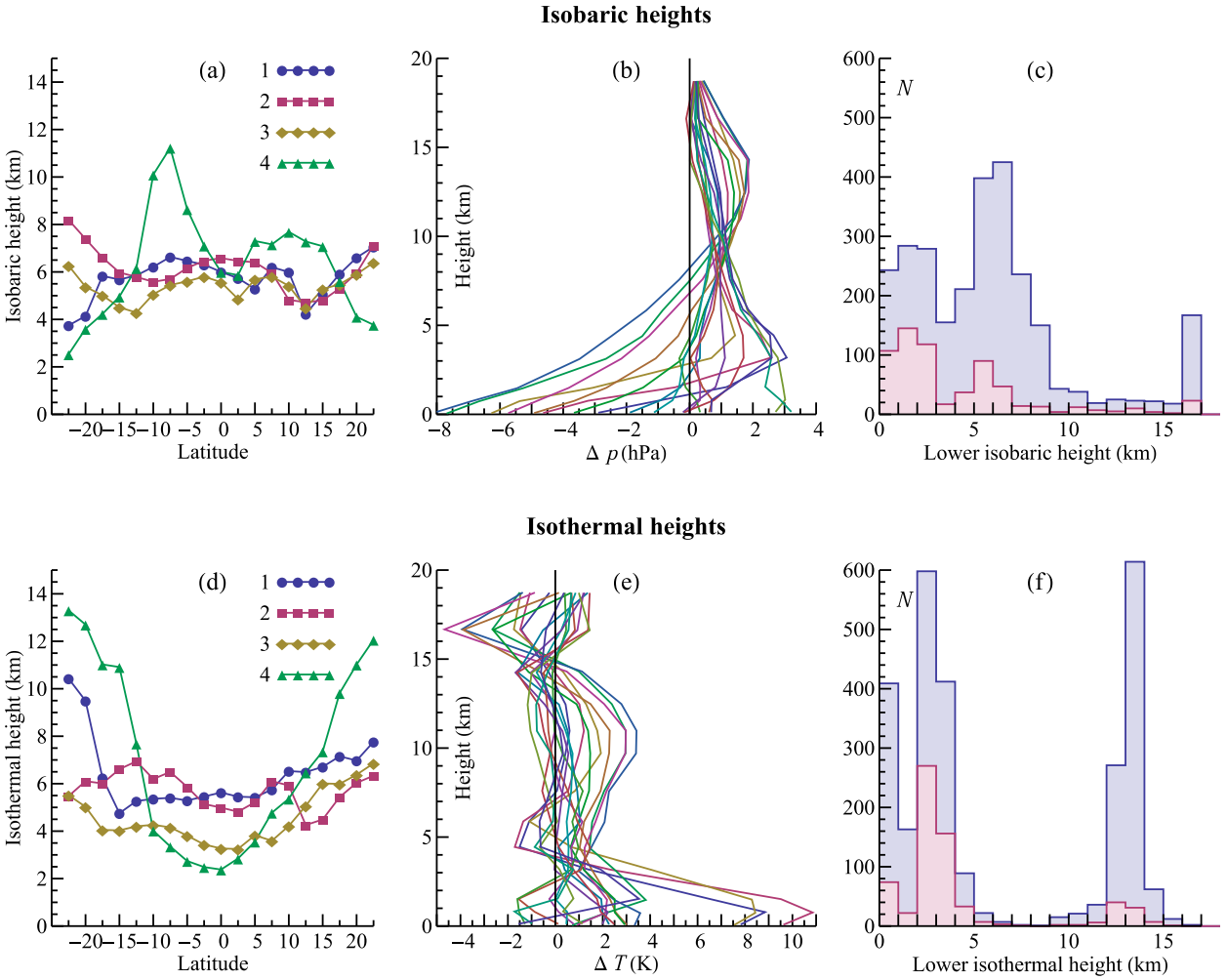

FIG. 5. (a)–(c) Isobaric and (d)–(f) isothermal heights in the tropical troposphere. (a),(d): zonal averages of isobaric and isothermal heights defined as follows: 1) minimum height where local pressure (temperature) coincides with the mean pantropical pressure (temperature) at this height (blue); 2) minimum height where local pressure (temperature) coincides with the mean zonal pressure (temperature) at this height (magenta); 3) minimum height where local zonal gradient of pressure (temperature) is zero (gold); and 4) minimum height where local meridional gradient of pressure (temperature) is zero (green). All local pressure and temperature values are annual means. (b),(e) Vertical profiles of the differences between the mean pantropical profile of pressure (temperature) in July and the profile of pressure (temperature) for 18 individual grid points at 20°N that are spaced by 20° longitude starting from 0°. Note the difference between isobaric heights 1 and 2: individual profiles coincide with each other at a different height (around 10 km) than they coincide with the pantropical mean profile. Frequency distribution of (c) isobaric and (f) isothermal heights 1; the inner histogram shows the distribution of land values only and the outer histogram shows all values.

the troposphere (Bayr and Dommenget 2013). Apparently, in the presence of two isobaric heights the $\Delta p_s/\Delta T_a$ ratio cannot be a linear function of z_e. Indeed, we have shown that an additional parameter is required: the isothermal height z_i. The resulting dependence of $\Delta p_s/\Delta T_a$ on the isobaric height is quadratic, not linear [Eq. (19)].

Isothermal height z_i characterizes the thermal structure of the troposphere. In the limit of very large z_i the ratio $\Delta p_s/\Delta T_s$ (as well as $\Delta p_s/\Delta T_a$) does not depend on z_i, but only on isobaric height z_e [Eqs. (16) and (20)]. If z_e is given, Δp_s depends only on surface temperature contrasts. This fact apparently facilitated interpretation of surface pressure contrasts as *determined* by surface temperature (Lindzen and Nigam 1987; Sobel and Neelin 2006; An 2011). For example, Sobel and Neelin (2006, p. 324) in their discussion of the model of Lindzen and Nigam (1987) noted that surface temperature determines temperature in the atmospheric boundary layer, which, in turn, determines surface pressure via a hydrostatic relationship. Indeed, if the lapse rate does not vary in the horizontal plane, $z_i = +\infty$ and there is a direct proportionality between Δp_s and T_s (and T_a).

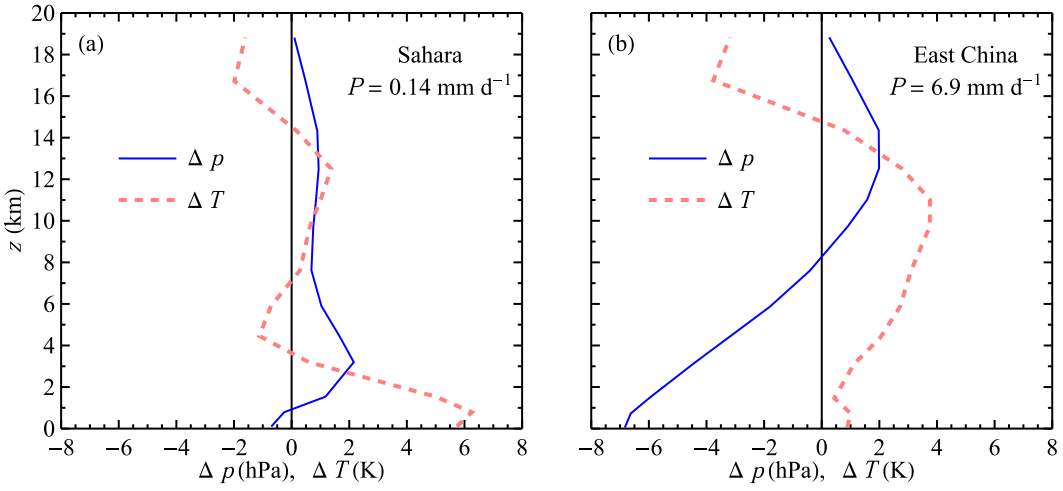

FIG. 6. Vertical profiles of air pressure and temperature differences between the zonal mean (20°–30°N) in July and (a) the Sahara (20°–30°N, 0°–20°E) and (b) eastern China (20°–30°N, 100°–120°E); P is precipitation in July in these regions (mm day^{-1}).

However, while in the real atmosphere z_i is on average relatively large, this is not because the release of latent heat does not matter. Rather, it is the release of latent heat that elevates the isothermal height by diminishing the difference in the mean tropospheric lapse rate between the warmer and colder surface areas. An illustration is shown in Fig. 6, which compares pressure and temperature profiles in the Sahara and eastern China in July each with the zonal mean profile. One can see that in the dry Sahara the isothermal height is very small while at the same latitude in eastern China (during the monsoon) it is typically higher. When z_i is not very large but comparable to z_e, it has a crucial impact on the relationship between pressure and temperature [Eq. (19)].

Figure 6 also illustrates how in moist regions there is a larger surface pressure drop compared to the zonal mean than in dry regions. For example, with the Sahara surface being almost 6 K warmer than the zonal mean, $\Delta T_s = 6$ K, the surface pressure is only 0.7 hPa lower than the zonal mean, $\Delta p_s = -0.7$ hPa. In eastern China for an insignificant $\Delta T_s = 1$ K we have a significant surface pressure drop $\Delta p_s = -7.0$ hPa compared to the zonal mean.

We have shown that the relationship between $\Delta p_s/\Delta T_a$ (as well as of $\Delta p_s/\Delta T_s$) is sensitive to the values of z_e and z_i (Fig. 3). This sensitivity has not been previously explored. For example, at $z_i = 10$ km, which is the value adopted by Lindzen and Nigam (1987), a 15% change in the upper z_e from 17 to 20 km leads to a complete disappearance of the dependence of Δp_s on both ΔT_s and ΔT_a. Thus any assumed approximate constancy of the upper isobaric height z_{e2} is too far from reality to determine the $\Delta p_s/\Delta T_a$ ratio [contrary to the suggestions of Bayr and Dommenget (2013)]. The sensitivity to the lower isobaric height z_{e1} is less marked (Fig. 3b), but at the same time z_{e1} varies proportionally more in space than does z_{e2}: z_{e1} varies from a few hundred meters over land to over 6 km over the ocean (Fig. 5c). Thus neither z_{e1} nor z_{e2} can usefully constrain predictions of $\Delta p_s/\Delta T_a$. With several different peaks, different values for land and ocean and mean values depending on latitude (Fig. 5a,d) the isobaric and isothermal heights cannot be specified from independent physical considerations. Rather, they are themselves dictated by the dynamic relationships between pressure and temperature.

We have emphasized how isobaric height links sea level pressure contrasts to the pressure contrasts in the troposphere [Eq. (22)]. If the isobaric height is unknown, so are the surface pressure contrasts. Unlike the tropospheric pressure contrast, the surface pressure contrasts cannot be determined from consideration of temperature gradients alone. This highlights a major problem for the theory of atmospheric circulation. Having set a temperature gradient, one can easily find tropospheric pressure gradients and, consequently, the geostrophic winds in the troposphere. However, what type of circulation can be generated in the low-level atmosphere remains uncertain. To simulate low-level winds generated by differential heating, one has to specify the dynamic interaction between the upper and lower atmosphere (i.e., the turbulent friction). Depending on the adopted parameterization, one and the same temperature gradient can be modeled to produce drastically different low-level winds. For example, for an axisymmetric general atmospheric circulation different assumptions regarding friction yield diverse

results from complete absence of any low-level circulation to negligible meridional circulation to circulations close to the observed (e.g., Held and Hou 1980; Schneider 2006). Through parameterization of turbulence, models of more local circulations driven by differential heating adopt as granted the basic parameters of the larger-scale circulations into which they are embedded (e.g., Smagorinsky 1953; Pielke 1981; Curry 1987). While optimized to provide an adequate description of the relevant processes, such models would yield different results if those basic parameters change.

A relevant illustration of these ideas is provided by the model of Lindzen and Nigam (1987). They investigated how low-level winds depend on the isobaric height z_e in their model, where the boundary layer height was assumed to be equal to z_e. In the limit $z_e \rightarrow 0$ the surface pressure gradients disappear [Eq. (16)] and the low-level winds should vanish. Contrary to this expectation, Lindzen and Nigam (1987) found little dependence of the meridional winds (and moisture convergence) on z_e in their model. A smaller z_e expectedly produced weaker surface pressure gradients, but it also produced a proportionally larger damping coefficient $\epsilon \equiv C_D|V_c|/z_e$, where C_D is a constant and V_c is a typical wind speed at z_e. As a result of a weaker meridional pressure gradient, the zonal wind did decrease proportionally to the surface pressure gradient. However, the meridional wind proportional to the product of zonal wind and the damping coefficient ϵ [Lindzen and Nigam 1987; see their Eq. (12a)] did not change much. Here the decrease in pressure gradient was offset by an increase in the damping coefficient ϵ, such that the low-level air convergence remained approximately independent of z_e (and, hence, of surface pressure gradients).[4]

Thus any answer to the question ''what happens in the lower atmosphere?'' depends much more on how turbulence is parameterized than on the magnitude of any temperature contrasts. Since turbulent friction and the dissipative power of atmospheric circulation are directly linked, finding constraints on dissipative power can contribute to our understanding of low-level circulation and moisture convergence (Makarieva et al. 2013a,b).

We have seen that the relationship between p_s and T_a in the tropics shown in Fig. 3 of Bayr and Dommenget (2013) is mainly determined by the properties of the tropical atmosphere around 20° latitude as well as by its zonally averaged properties (Fig. 4c). Thus to explain why the ratios between sea level pressure and temperature contrasts have their observed magnitudes we have to explain why the Hadley and Walker circulations are characterized by those pressure and temperature contrasts. Other processes, including seasonal variation and the observed long-term relative p_s and T_a changes as in Fig. 12 of Bayr and Dommenget (2013), appear to preserve the vertical structure of the atmosphere set by the main dynamic drivers of the circulation. In other words, if we knew why there is an ~10-hPa pressure contrast for every ~10°C tropospheric and surface temperature contrast in Hadley cells we would be able to determine the isobaric heights and thus understand why the tropical troposphere is about 16 km and not, say, 10- or 25-km high as well as why a local temperature increase leads to a local sea level pressure drop of a given magnitude.

In the past two physical drivers of low-level circulation have been proposed and examined by researchers: surface heating and the release of latent heat (Gill 1980; Lindzen and Nigam 1987; Neelin 1989; Sobel and Neelin 2006; Back and Bretherton 2009; An 2011). A distinct physical process was recently described. Horizontal transport of moisture with its subsequent condensation and precipitation away from the point where it evaporated produces pressure gradients due to the changing concentration of water vapor as the air moves from the evaporation to condensation area (Makarieva et al. 2013b, 2014a,b). Pressure is greater where water vapor is added and lower where it is removed from the air column. Understanding the relative contributions of these processes will guide our predictions of local pressure and circulation changes. We believe that the analysis of pressure–temperature relationships initiated by Bayr and Dommenget (2013) can shed light on the relative strength of the contributing processes if these are studied together with the moisture contrasts.

[4] This independence of the meridional wind on z_e resulted from the assumed constancy of V_c and, hence, from the inverse proportionality between the damping coefficient and the isobaric height. In the real atmosphere the height of boundary layer h_b is much smaller than the isobaric height, $h_b \sim 1\,\text{km} \ll z_e$, especially over the ocean (Fig. 5c). Because of this, pressure gradients at the top of the boundary layer are determined by the surface pressure gradients and close to them. Since at the top of the boundary layer winds are approximately geostrophic (Back and Bretherton 2009), this means that the geostrophic wind speed V_c at the top of the boundary layer (which is used in the determination of the damping coefficient) is approximately proportional to the surface pressure gradient. Consequently, it must decrease with decreasing z_e . In the result, with decreasing z_e (decreasing surface pressure gradient), surface winds and moisture convergence should decline as well. Note also that z_e can itself be considered as a function of pressure gradients.

Acknowledgments. We sincerely thank Dr. T. Bayr and Dr. D. Dommenget and the reviewers for constructive critical comments. This work was partially supported by Russian Scientific Foundation under Grant 14-22-00281.

APPENDIX

Relationship between T_s and T_a

The relationship between surface temperature T_s and the mean temperature $T_a(Z)$ of the atmospheric column below Z can be derived from Eq. (9) and the hydrostatic Eq. (5):

$$T_a(Z) \equiv \frac{\int_0^Z T(Z)\rho\, dZ}{\int_0^Z \rho\, dZ} = \frac{T_s}{1+c}\,\frac{1-e^{-cZ}e^{-Z}e^{-cZ^2/2}}{1-e^{-Z}e^{-cZ^2/2}}, \tag{A1}$$

where $Z \equiv z/h_s$ and $cZ \ll 1$.

Expanding Eq. (A1) over c and keeping the linear term we have

$$T_a = T_s\left[1 - c\left(1 - \frac{Z}{e^Z - 1}\right)\right]. \tag{A2}$$

Taking the derivative of Eq. (A2) over T_s and c we obtain

$$dc = \frac{db - dn}{1 - Z/(e^Z - 1)} \quad \text{and} \quad dn \equiv \frac{dT_a}{T_a}. \tag{A3}$$

For the height of the tropical troposphere $z = H = 16.5\,\text{km}$, $T_s = 298\,\text{K}$, and $\Gamma = 6.1\,\text{K km}^{-1}$ we have $Z = 1.9$, $c = 0.18$, and $1 - Z/(e^Z - 1) = 0.66$ and obtain from Eqs. (A2) and (A3)

$$T_a = 0.88T_s, \quad db = dn + 0.66dc, \quad \text{and}$$
$$\frac{dT_s}{dT_a} = \frac{1}{0.88}\left(1 + 0.66\frac{d\Gamma}{dT_a}\frac{T_a}{\Gamma_g}\right). \tag{A4}$$

The mean tropospheric $\overline{T_a} = 262\,\text{K}$ in the tropics estimated from Eq. (A4) is identical to the annual tropical mean $\overline{T_a} = 262\,\text{K}$ (22.5°S–22.5°N) that we estimate from the TTT data of Mears and Wentz (2009) and close to $\overline{T_a} = 263.6\,\text{K}$ cited by Bayr and Dommenget (2013).

REFERENCES

Acharya, N., S. C. Kar, U. C. Mohanty, M. A. Kulkarni, and S. K. Dash, 2011: Performance of GCMs for seasonal prediction over India—A case study for 2009 monsoon. *Theor. Appl. Climatol.,* **105,** 505–520, doi:10.1007/s00704-010-0396-2.

An, S.-I., 2011: Atmospheric responses of Gill-type and Lindzen–Nigam models to global warming. *J. Climate,* **24,** 6165–6173, doi:10.1175/2011JCLI3971.1.

Back, L. E., and C. S. Bretherton, 2009: On the relationship between SST gradients, boundary layer winds, and convergence over the tropical oceans. *J. Climate,* **22,** 4182–4196, doi:10.1175/2009JCLI2392.1.

Bayr, T., and D. Dommenget, 2013: The tropospheric land–sea warming contrast as the driver of tropical sea level pressure changes. *J. Climate,* **26,** 1387–1402, doi:10.1175/JCLI-D-11-00731.1.

Curry, J., 1987: The contribution of radiative cooling to the formation of cold-core anticyclones. *J. Atmos. Sci.,* **44,** 2575–2592, doi:10.1175/1520-0469(1987)044<2575:TCORCT>2.0.CO;2.

Gill, A. E., 1980: Some simple solutions for heat-induced tropical circulation. *Quart. J. Roy. Meteor. Soc.,* **106,** 447–462, doi:10.1002/qj.49710644905.

Hagemann, S., C. Chen, J. O. Haerter, J. Heinke, D. Gerten, and C. Piani, 2011: Impact of a statistical bias correction on the projected hydrological changes obtained from three GCMs and two hydrology models. *J. Hydrometeor.,* **12,** 556–578, doi:10.1175/2011JHM1336.1.

Held, I. M., and A. Y. Hou, 1980: Nonlinear axially symmetric circulations in a nearly inviscid atmosphere. *J. Atmos. Sci.,* **37,** 515–533, doi:10.1175/1520-0469(1980)037<0515:NASCIA>2.0.CO;2.

Huang, P., S.-P. Xie, K. Hu, G. Huang, and R. Huang, 2013: Patterns of the seasonal response of tropical rainfall to global warming. *Nat. Geosci.,* **6,** 357–361, doi:10.1038/ngeo1792.

Johnson, R. H., T. M. Rickenbach, S. A. Rutledge, P. E. Ciesielski, and W. H. Schubert, 1999: Trimodal characteristics of tropical convection. *J. Climate,* **12,** 2397–2418, doi:10.1175/1520-0442(1999)012<2397:TCOTC>2.0.CO;2.

Kalnay, E., and Coauthors, 1996: The NCEP/NCAR 40-Year Reanalysis Project. *Bull. Amer. Meteor. Soc.,* **77,** 437–471, doi:10.1175/1520-0477(1996)077<0437:TNYRP>2.0.CO;2.

Landau, L. D., and E. M. Lifshitz, 1987: *Fluid Mechanics*. Vol. 6, *Course of Theoretical Physics,* 2nd ed., Butterworth-Heinemann, 539 pp.

Lindzen, R. S., and S. Nigam, 1987: On the role of sea surface temperature gradients in forcing low-level winds and convergence in the tropics. *J. Atmos. Sci.,* **44,** 2418–2436, doi:10.1175/1520-0469(1987)044<2418:OTROSS>2.0.CO;2.

Makarieva, A. M., V. G. Gorshkov, A. V. Nefiodov, D. Sheil, A. D. Nobre, P. Bunyard, and B.-L. Li, 2013a: The key physical parameters governing frictional dissipation in a precipitating atmosphere. *J. Atmos. Sci.,* **70,** 2916–2929, doi:10.1175/JAS-D-12-0231.1.

——, ——, D. Sheil, A. D. Nobre, and B.-L. Li, 2013b: Where do winds come from? A new theory on how water vapor condensation influences atmospheric pressure and dynamics. *Atmos. Chem. Phys.,* **13,** 1039–1056, doi:10.5194/acp-13-1039-2013.

——, ——, and A. V. Nefiodov, 2014a: Condensational power of air circulation in the presence of a horizontal temperature gradient. *Phys. Lett.,* **378A,** 294–298, doi:10.1016/j.physleta.2013.11.019.

——, ——, D. Sheil, A. D. Nobre, P. Bunyard, and B.-L. Li, 2014b: Why does air passage over forest yield more rain? Examining the coupling between rainfall, pressure, and atmospheric

moisture content. *J. Hydrometeor.,* **15,** 411–426, doi:10.1175/JHM-D-12-0190.1.

Marengo, J. A., 2006: On the hydrological cycle of the Amazon Basin: A historical review and current state-of-the-art. *Rev. Bras. Meteor.,* **21,** 1–19.

Mears, C. A., and F. J. Wentz, 2009: Construction of the Remote Sensing Systems V3.2 atmospheric temperature records from the MSU and AMSU microwave sounders. *J. Atmos. Oceanic Technol.,* **26,** 1040–1056, doi:10.1175/2008JTECHA1176.1.

Neelin, J. D., 1989: On the interpretation of the Gill model. *J. Atmos. Sci.,* **46,** 2466–2468, doi:10.1175/1520-0469(1989)046<2466:OTIOTG>2.0.CO;2.

Pielke, R. A., 1981: An overview of our current understanding of the physical interactions between the sea- and land-breeze and the coastal waters. *Ocean Manag.,* **6,** 87–100, doi:10.1016/0302-184X(81)90030-5.

Schneider, T., 2006: The general circulation of the atmosphere. *Annu. Rev. Earth Planet. Sci.,* **34,** 655–688, doi:10.1146/annurev.earth.34.031405.125144.

Smagorinsky, J., 1953: The dynamical influence of large-scale heat sources and sinks on the quasi-stationary mean motions of the atmosphere. *Quart. J. Roy. Meteor. Soc.,* **79,** 342–366, doi:10.1002/qj.49707934103.

Sobel, A. H., and J. D. Neelin, 2006: The boundary layer contribution to intertropical convergence zones in the quasi-equilibrium tropical circulation model framework. *Theor. Comput. Fluid Dyn.,* **20,** 323–350, doi:10.1007/s00162-006-0033-y.

Thorpe, A. J., H. Volkert, and M. J. Ziemiański, 2003: The Bjerknes circulation theorem: A historical perspective. *Bull. Amer. Meteor. Soc.,* **84,** 471–480, doi:10.1175/BAMS-84-4-471.